NIH Public Access
Author Manuscript
Carbohydr Res. Author manuscript; available in PMC 2009 July 21.

Published in final edited form as:
Carbohydr Res. 2008 July 21; 343(10-11): 1594–1604. doi:10.1016/j.carres.2008.05.003.

Varied Presentation of the Thomsen-Friedenreich Disaccharide Tumor-Associated Carbohydrate Antigen on Gold Nanoparticles

Andreas Sundgren and **Joseph J. Barchi Jr.***
Laboratory of Medicinal Chemistry and, Center for Cancer Research, National Cancer Institute at Frederick, 376 Boyles Street, Frederick, Maryland, 21702, USA

Abstract

Three-dimensional self-assembled monolayers of gold coated with the Thomsen-Friedenreich antigen (TF_{ag}) disaccharide (β-Gal*p*-(1→3)-Gal*p*NAc) in a variety of presentations have been prepared and characterized. Anomalies in the size distribution of our originally synthesized TF_{ag}-bearing nanoparticles as shown in dynamic light scattering experiments prompted us to explore the effect of antigen density on the uniformity of the particles. Gold nanoparticles containing a range of densities "diluted" with copies of the PEG-thiol spacer unit showed that lower antigen density affords more uniform particles. We also wanted to study the constitution of the actual antigen by synthesizing nanoparticles not only with the linker-extended disaccharide, but within the context of the surrounding peptide sequence where it may be presented *in vivo*. The synthesis of thiol-containing TF_{ag}-containing glycopeptides from a mucin peptide repeating unit were prepared, assembled into gold nanoparticles and their physical properties evaluated. These novel multivalent tools should prove extremely useful in exploring the binding properties and immune response to this important carbohydrate antigen.

Keywords

Thomsen-Friedenreich antigen; Gold nanoparticles; Glycopeptides; Immunogen

1. Introduction

Spurred by recent advances in technology development, there has been a surge in the design, development and the use of nanoscale platforms for many areas of medical research. Various materials (such as gold[1], iron oxide[2] and semiconductor materials[3]) can be employed to form self-assembled structures that can be coated with organic agents or biomacromolecules. These novel nanoparticles (NP's) have intriguing physical properties that may be related to their core materials and nanometer size ranges, as well as the chemistry of the coating itself. The field of carbohydrate chemistry has benefited from this technology, as many platforms allow the presentation of multiple copies of a particular molecule (or many different molecules) on their surface, yielding multivalent constructions that can be used to study and/or interfere with carbohydrate-protein interactions. Hence, "glyconanotechnology"[4–8] is a burgeoning field and there are now a host of published examples of glyconanoparticles (GNP's) that have shown

Address Correspondence to: Joseph J Barchi Jr. Ph.D., National Cancer Institute Frederick, 376 Boyles Street, PO Box B, Building 376 Room 209, Frederick, MD 21702, 301-846-5905, 301-846-6033 (FAX), barchi@helix.nih.gov.

Publisher's Disclaimer: This is a PDF file of an unedited manuscript that has been accepted for publication. As a service to our customers we are providing this early version of the manuscript. The manuscript will undergo copyediting, typesetting, and review of the resulting proof before it is published in its final citable form. Please note that during the production process errors may be discovered which could affect the content, and all legal disclaimers that apply to the journal pertain.

NIH-PA Author Manuscript
NIH-PA Author Manuscript
NIH-PA Author Manuscript

NIH-PA Author Manuscript

NIH-PA Author Manuscript

NIH-PA Author Manuscript

strong potential to act as extremely useful tools in glycan science. One of the most widely used platforms that have often been "sugar-coated" is that which employs spherical self assembled monolayers of gold. These gold NP's have a strong affinity for organic thiols and their synthesis has been refined to where highly stable and relatively monodispersed particles can be rapidly produced through simple reduction of gold salts in the presence of a molecule of choice tethered appropriately to a terminal mercapto group.[9] Thus, mono- and oligosaccharides have been displayed on the surface of gold NP's and shown to have provocative characteristics compared with their monovalent counterparts.[10] In addition, carbohydrates have been attached on quantum dots[11–15] for cell imaging applications and on magnetic NP's[16] for differential separation of bacterial strains.

Our interest in this area is targeted to the synthesis of GNP's with tumor associated carbohydrate antigens[17–19] (TACA's) on their surface. TACA's are aberrantly expressed carbohydrate units found on the cell surface of tumors that derive from the differences in the way glycans are processed in malignant cells compared to normal phenotypes. Our rationale for the design of these particles was twofold: 1) They have the potential to be used as a novel vaccine platform[20] to elicit an immune response *in vivo*, or, 2) They could be useful inhibitors of well-known protein carbohydrate interactions in which specific TACA's are involved. For these reasons we concentrated on the Thomsen-Friedenreich disaccharide (TF_{ag})[21,22], a human TACA present primarily in carcinomas but rarely expressed in normal tissues.[23] This antigen has been the subject of many studies attempting to design immunogens or vaccine platforms targeted to this TACA.[24–26] In addition, tumors displaying the TF_{ag} metastasize through a specific interaction with endothelial cell-derived galectin-3 (Gal-3).[27,28] Both adhesion to Gal-3 and cell growth are inhibited by TF_{ag} function-blocking or anti galectin-3 antibodies. Another report corroborated the importance of the TF_{ag}–Gal-3 interaction by showing that Gal-3 interacts with the cancer-associated mucin MUC1 via TF_{ag}.[29] This interaction caused a polarization of MUC1 on the cell surface revealing epithelial adhesion molecules that are otherwise concealed by MUC1, thus promoting cancer cell adhesion to the endothelium. The fact that TF_{ag} is covalently attached to the peptide backbone of MUC1, suggests that the surrounding peptide sequence is part of the antigen that is recognized by the immune system, and hence synthetic glycopeptides may be better immunogens than the "naked" dissacharide.

We mentioned in our earlier report[30] that TF_{ag}-coated GNP's could inhibit lung metastasis in the murine 4T1 breast cancer model. The details of this work were never published since we unfortunately were not able to reproduce the original result in several subsequent studies using different nanoparticle concentrations and control experiments with particles coated simply with hydroxyl-terminated linker groups (*vide infra*). Although we showed that TF_{ag}-coated GNP's agglutinated TF_{ag}-specific antibodies, TF_{ag}-coated GNP's were unable to inhibit TF_{ag}-specific antibody binding to immobilized BSA-conjugated TF_{ag} (Barchi, Rittenhouse-Olson, Heimburg, Sundgren, unpublished results). A closer examination revealed that the TF_{ag}-coated GNP's were polydispersed (non-uniform size distribution) in solution by dynamic light scattering (DLS) experiments (*vide infra*). We reasoned that this may be the source of the problems with our *in vivo* experiments and prompted us to refine the synthesis of the NP's to increase their mondispersity and attempt to determine the causes of the aforementioned non-uniformity. In addition, we synthesized the antigen in different forms including within a tumor-associated glycopeptide construction from a mucin protein (MUC4).

2. Results and Discussion

Our synthesis of TF_{ag}-coated GNP's employed the reduction of gold salts by $NaBH_4$ in the presence of specific carbohydrate-linked thiols.[31,32] This method has been utilized in many GNP reports cited above and the results, in general, have been quite successful. In our previous

NIH-PA Author Manuscript

NIH-PA Author Manuscript

NIH-PA Author Manuscript

work, we synthesized TF_{ag}-coated GNP's with approximately 90 sugar units on the gold surface **1** along with the unnatural β-analogue **2** to compare the quality and properties of these particles with the α-linked GNP's. For our *in vivo* studies, we had prepared the control particles **3**, which displayed simply the linker molecule where the TF_{ag} disaccharide is essentially substituted with a simple hydroxyl group (Figure 1).

The synthesis of the pentenyl-hexaPEG linker and TF_{ag}-linked thiol was as described previously.[30] The GNP's and linker-coated particles were purified by ultrafiltration and analyzed by transmission electron microscopy (TEM), NMR spectroscopy, elemental analysis and dynamic light scattering (DLS). The core diameter of the GNP's **1** and **2** was in the 5–7 nm range by TEM measurements, whereas NP's **3** with simply the linker were slightly larger and somewhat more polydispersed but in solution looked superior to the disaccharide-bearing particles (Figure 2). In comparing the GNP's **1–3** by DLS, the α-linked TF_{ag} particles **1** were the least uniform and their hydrodynamic diameter (HDD) was also twice as large as β-linked TF_{ag} GNP's when volumes are considered (Figure 2).

Initially, our hypothesis was that the anomeric stereochemistry of the sugar could cause problems in the self-assembly process of the nanoparticles. Very few α-linked sugars have been coated on gold nanoparticles.[33] To our knowledge, only one group has synthesized α-linked disaccharides on gold and they showed that different aggregation properties were observed when comparing α and β-linked disaccharide-coated particles.[34,35] If the directionality of the sugar is angled differently in the α- and β-linked GNP's and this is the source of aberrations in the self-assembly process, reducing the carbohydrate density on the surface may facilitate the production of more uniform particles yielding a tighter distribution of sizes. Scheme 1 outlines the synthesis of GNP's with various ratios of carbohydrate ligand to underivatized linker thiol used in the reaction mixture. As the density of the carbohydrate is lowered on the particle surface, the size distribution also improves (see Supporting Information for DLS data on particles **6–9**). In addition, the optimum uniformity is observed for the particles prepared where a 5:1 linker-to-sugar ratio is used (compound **10**). This method is being used by us for the comparison of various particles with different passivating agents and surface coatings. For example, we have prepared simple β-galactose-coated GNP's from compounds where the linker-to-sugar ratio was either 0:1, 1:1 or 5:1. Microscopy and sizing data also showed that the 5:1 linker-to-sugar particles have the most uniform size by both DLS and TEM analysis and the ability for these to inhibit or promote HIV fusion to mammalian cells changes with carbohydrate density (unpublished results).

The scientific literature is replete with reviews about TACA's along with suggestions on the exact constitution of the actual antigen "structures". Many (including us) believe the recognition element of a specific glycoprotein-based TACA includes either the amino acid or local peptide sequence to which it is attached in is natural cellular context. In addition, this "natural" antigen should elicit a more powerful immune response in synthetic vaccine preparations since it should more closely resemble the conformation displayed in vivo. Recent work has shown that nanoparticle platforms have the potential to act as single-[36,37] or multi-component[20] vaccine scaffolds. We thus extended the antigen "structure" to the TF_{ag} coupled to specific mucin peptides. Mucins are very large proteins that act as a lubricant and can protect the cell surface from outside insult. The long protein backbone is comprised of many repeating motifs of between ~16–22 amino acids that contain several serine and threonine residues of which the majority are glycosylated.[38] This serves to "extend" the protein backbone straight out from the cell surface, and the inter-digitation of the mucin molecules forms a protective barrier as part of the glycocalyx. Several mucins are overexpressed in various cancers; structures related to both the carbohydrate and the peptide backbone of mucins have been employed in antitumor vaccines strategies. We chose the 16-amino acid repeating unit of MUC4 (Figure 3), the primary mucin found on adenocarcinomas of the pancreas,[39–42] for

NIH-PA Author Manuscript

NIH-PA Author Manuscript

NIH-PA Author Manuscript

our studies to prepare glycopeptide-coated nanoparticles (GPNP's). The Kunz group had previously synthesized several glycopeptides of MUC4 by solid phase peptide synthesis for use in immunological studies. We followed similar procedures to make a repertoire of glycopeptides for assembly on gold particles.

We have synthesized glycopeptides with the TF_{ag} at two separate positions and developed appropriate linker chemistry for the synthesis of GPNP's (Scheme 2).

SPPS of the peptides proceeded smoothly for the majority of the coupling reactions. We employed Fmoc chemistry using a mixture of HOBt and HBTU for activation. Synthesis was performed mostly in the automated mode on a peptide synthesizer. The glycoamino acid, however, was coupled manually and depending on the position of the sugar unit in the peptide sequence, specific conditions were needed to affect efficient coupling. The two glycopeptides we report on here had the TF_{ag} at the 6^{th} and 10^{th} threonine residues (Figure 3). We prepared the appropriately functionalized control peptide (without a covalently attached carbohydrate) attached to the linker unit for self assembly onto gold particles. The linker strategy is one that deserves mention, since this can be a critical component in the production of NP's. The glycopeptide linker described here incorporated a PEG unit and a fatty portion which can potentially facilitate packing at the surface. Linkers consisting solely of PEG units were difficult to couple to the peptide and did not self assemble efficiently. An extender glycine amino acid was added to bolster the reactivity of the carboxylate toward coupling with the amino group of the peptide. The commercially available *N*-Fmoc-1-amino-3,6,9,12,15,18-hexaoxahenicosan-21-oic acid was reacted according to Scheme 2 to yield the linker **17** which was coupled to the peptide on resin. Deprotection of the acetate groups was also accomplished most efficiently while attached to the resin with hydrazine/ethanol. Coupling of the glycoamino acids was performed with HOBt–diisopropylcarbodiimide (DIPCDI), and although efficient, was slow and required extended reaction times and additional activating reagents to reach completion. Experimentation with microwave catalysis to improve the yield and increase the rate of these coupling steps is in progress. Scheme 3 outlines the method for the preparation of GPNP's **20–22** from the compounds **12** and **13**.

In addition to preparing the peptide-bearing particles **19** and GPNP's **20** and **21**, we prepared the "diluted" particles with a 1:5 ratio of glycopeptide to linker (**22**) along with another "control" particle containing the linker alone (**23**). It was necessary to modify the linker **17** used in the synthesis of **23** by extension with an ethanolamine tail to produce **18** for the preparation of particles that expose simple hydroxyl groups on their surface similar to our approach for linker-coated NP's **3**. The rationale for producing two "control" particles (**19** and **23**) is to be able to dissect the effects of the sugars, the peptide backbone and the linker on the recognition of the GPNP's. Physical characterization of particles **19–23** followed similarly as for the GNP's above. An estimate as to the number of copies of glycopeptide exposed on the GPNP's was made from elemental analysis and core diameters that estimate the number of gold atoms in the particle composition.[43] The glycopeptides **20** and **21** contained ca. 180 copies of ligand while for the peptide alone (**19**) there are an estimated 220 copies. The peptide and glycopeptide-conjugated gold particles all looked very uniform by TEM analysis (Figure 4). As has been shown in several past reports including from our laboratory, NMR of the GNP's or GPNP's in water show nearly all signals that are evident in the monomeric ligands, but broadened by the high molecular weight and changes to relaxation times in the NP's (data not shown). A surprising discovery during this work was that, even with identical synthetic procedures used throughout to prepare NP's, uniformity was dictated by the surface chemistry and could not be predicted a priori. Hence, the disaccharide-coated NP's that were prepared typically showed polydispersity unless "diluted" with interstitial spacer PEG linkers to reduce the saccharide density on the surface of the particle. Glycopeptides were consistently more uniform by microscopic analysis, but in all particles that we have made to date, DLS analysis

NIH-PA Author Manuscript

NIH-PA Author Manuscript

NIH-PA Author Manuscript

shows intensity bands in the range of 50–150 nm. These usually disappear on conversion of these intensity maps to volumes or when the particles are first filtered through membranes that exclude all material above 0.1 um, indicating that although there may be particles that are much larger in hydrodynamic diameter (HDD) and scatter light efficiently, their actual number is quite low and the bulk of the particles are in the 7–11 nm HDD range. We are now in the process of testing these novel particles in several bioassays and the results will be reported in due course.

3. Conclusions and Summary

Gold nanoparticles bearing the Thomsen Friedenreich antigen at different densities and in different contexts have been prepared and characterized. Sizing data showed that certain sugar presentations result in the assembly of particles that may have reasonable uniformity in their gold core diameters by TEM analysis, but they can be polydispersed and “non-uniform” in solution. Glycopeptide-coated nanoparticles result in more uniform particles as seen by TEM analysis, however, GNP’s and GPNP’s contain some larger size elements that could be a consequence of either aberrations in the self assembly process or aggregation events. An important conclusion gleaned from this work is that nanoconstructions with various surface chemistries may display very different behavior when comparing microscopy to sizing measurements in solution. By comparing measurements performed in various milieus (water, 10 mM NaCl, PBS, data not shown), it is evident that each particle has their own individual properties when exposed to different solutions. This could have important consequences when studying these particles in a cellular or in vivo context. Subsequent reports will outline in detail the “idiosyncrasies” of each GNP(GPNP) and how these relate to their biological activity and therapeutic potential.

3. Experimental

Flash column chromatography (FCC) was performed using RediSep® silica columns on a CombiFlash® Companion® employing solvent polarity gradient (hexane → ethyl acetate). Reversed phase chromatography was performed on 900 mg Alltech® Maxi-Clean™ C_{18} Cartridges employing solvent polarity gradient (water → methanol) unless otherwise noted. Chemicals were purchased from Aldrich-Sigma (Milwaukee, WI) and used without further purification. NMR spectra were recorded on a Varian Inova 400 instrument with residual $CHCl_3$ (7.26 ppm) as the internal standard at frequencies of 399.74 MHz for ^1H and 100.51 MHz for ^{13}C. Assignments were based on gCOSY, TOCSY, ROESY, and ^{13}C/DEPT experiments. ^1H NMR data are tabulated in the order of multiplicity (s, singlet; d, doublet; dd, doublet of doublets; dt, double of triplets; t, triplet; q, quartet; m, multiplet; brs, broad signal), number of protons, and coupling constant(s) in Hertz. Specific optical rotations were determined using JASCO-P1010 polarimeter in 0.5 dm cuvette at 589 nm in chloroform. Five consecutive measurements were taken and the average value is reported. High resolution mass spectra were performed by Mass Spectrometry Facility at University of California, Riverside. Elemental analyses were performed by Atlantic Microlab, Inc., Norcross, GA and Galbraith Laboratories Inc., Knoxville, TN. Transmission electron micrographs were performed on a Hitachi H-7000 microscope equipped with a Gatan digital camera operating at 75 kV. A Malvern Zetasizer Nano ZS instrument (Southborough, MA) with back scattering detector was used for measuring the hydrodynamic size (diameter) in batch mode at 25 °C in a disposable low volume polystyrene microcuvette. Samples were measured at a concentration of 0.4 mg/mL or 0.2 mg/mL in both H_2O and PBS. Samples were filtered through a 0.1 μm filter before a minimum of ten measurements were made. Hydrodynamic size is reported as the intensity-weighted average over all size populations (Z-avg), and the volume-weighted average over a particular range of size populations corresponding to the most prominent peak in the % volume distribution (Vol-Peak).

NIH-PA Author Manuscript

NIH-PA Author Manuscript

NIH-PA Author Manuscript

3.1 General procedure for synthesis of gold nanoparticles

Thiol (1 eq.) and 58 mM $HAuCl_4$ (2.75 eq.) were added to water (10 mL/μmol thiol) and the obtained yellow solution was cooled to 0 °C. 0.1% $NaBH_4$ in water (1 mL/μmol thiol) was then added over 10 min where upon the color changed to red or purple over the first minute of addition. This solution was then stirred at 0 °C for 2 h and at rt for another 16 h. The solution was concentrated to about 5 mL, purified utilizing a Centriplus 30K filter and the obtained pure solution of the particles was lyophilized to obtain a dark-purple solid.

3.2. *t*-Butyl *N*-Fmoc-1-amino-21-oxo-3,6,9,12,15,18-hexaoxa-22-azatetracosan-24-oate (14)

N-Fmoc-1-amino-3,6,9,12,15,18-hexaoxahenicosan-21-oic acid (Available from NeoMPS Inc., San Diego, CA) (520 mg, 904 μmol) was dissolved in CH_2Cl_2 (3 mL) and cooled to 0 °C. A solution of 0.5 M HOBt in DMF (2.36 mL, 1.18 mmol) and DIPCDI (180 μL, 1.18 mmol) were added, this was stirred for 30 min at 0 °C after which H-Gly-O*t*Bu (152 mg, 904 μmol) was added. After stirring for 18 h, another portion of 0.5 M HOBt in DMF (4.70 mL, 2.35 mmol) and DIPCDI (362 μL, 2.35 mmol) were added and the reaction was stirred for another 48 h. The solvents were evaporated and the residue purified by column chromatography to give compound **14** (534 mg, 86%). ^{1}H NMR ($CDCl_3$): δ 1.46 (s, 9H, (CH_3)$_3$C)), 2.51 (t, 2H, *J* = 6.0 Hz), 3.40 (q, 2H, *J* = 5.6 Hz), 3.57 (t, 2H, *J* = 4.8 Hz), 3.62–3.64 (m, 20 H), 3.74 (t, 2H, *J* = 5.6 Hz), 3.92 (d, 2H, J = 5.6 Hz), 4.22 (t, 1H, *J* = 6.8 Hz), 4.40 (d, 2H, *J* = 6.8 Hz), 7.32 (dt, 2H, *J* = 1.2 Hz, *J* = 7.6 Hz, aromatic), 7.40 (dt, 2H, *J* = 0.8 Hz, *J* = 7.6 Hz), 7.61 (d, 2H, *J* = 7.6 Hz), 7.76 (d, 2H, *J* = 7.6 Hz); ^{13}C NMR ($CDCl_3$): δ 28.1, 36.7, 42.0, 47.3, 67.1, 70.30, 70.32, 70.5, 70.6, 81.6, 120.0, 125.1, 127.1, 127.7, 128.2, 129.1, 141.3, 144.0, 169.1, 171.7; HRMS $[C_{36}H_{52}N_2O_{11} + Na]^+$: calc. 711.347, found: 711.347.

3.3. 7-(thioacetyl)heptanoic acid (15)

Heptenoic acid (100 mg, 781 μmol) and AIBN (20 mg) were dissolved in MeOH (5 mL) containing thioacetic acid (200 μL). The flask was then irradiated with a 350 watt UV lamp for 6 h, concentrated and azeotroped with toluene. The residue was purified by column chromatography to yield compound **15** (133 mg, 84%). ^{1}H NMR ($CDCl_3$): δ 1.36–1.39 (m, 4H), 1.55–1.58 (m, 2H), 1.61–1.67 (m, 2H), 2.32 (s, 3H, CH_3COS), 2.35 (t, 2H, *J* = 7.6 Hz), 2.86 (t, 2H, *J* = 7.2 Hz); ^{13}C NMR ($CDCl_3$): δ 24.6, 28.5, 28.6, 29.1, 29.4, 30.8, 34.1, 180.2, 196.2. HRMS $[C_9H_{16}O_3S + Na]^+$: calc. 227.072, found: 227.072.

3.4. *tert*-Butyl 3,25-dioxo-6,9,12,15,18,21-hexaoxa-31-acetylthio-24-azahentriacontan-1-oate (16)

Compound **14** (518 mg, 753 μmol) was dissolved in CH_2Cl_2 (8 mL) and piperidine (3 mL) and the solution was stirred for 3 h, concentrated and azeotroped with toluene. The residue was filtered through a short silica column to give the crude amine (386 mg), which was dissolved in CH_2Cl_2 (5 mL) together with **14** (154 mg, 753 μmol) followed by addition of 0.5 M HOBt in DMF (1.96 mL, 979 μmol) and DIPCDI (150 (150 μL, 979 μmol). The reaction was stirred for 18 h, concentrated and the residue purified by column chromatography to give **16** (421 mg, 86%). ^{1}H NMR ($CDCl_3$): δ 1.33–1.37 (m, 4H), 1.46 (s, 9H, (CH_3)$_3$C)), 1.55–1.61 (m, 2H), 1.62–1.67 (m, 2H), 2.18 (t, 2H, *J* = 7.6 Hz). 2.33 (s, 3H, CH_3COS), 2.53 (t, 2H, *J* = 6.0 Hz), 2.86 (t, 2H, J = 7.2 Hz), 3.42–3.47 (m, 2H), 3.55 (t, 2H, *J* = 4.8 Hz), 3.62–3.64 (m, 22 H), 3.76 (t, 2H, *J* = 5.6 Hz), 3.93 (d, 2H, *J* = 5.6 Hz); Anal. Calcd for $C_{30}H_{56}N_2O_{11}S$: C 55.19; H 8.65; N 4.29, found: C 54.91; H 8.42; N 4.17.

3.5. 3,25-dioxo-6,9,12,15,18,21-hexaoxa-31-mercaptoheptanamido-24-azahentriacontan-1-oic acid (17)

Compound **16** (200 mg, 307 μmol) was dissolved in 90% TFA (5 mL) and the obtained solution was stirred for 40 min. The reaction was concentrated and the residue was purified by column

NIH-PA Author Manuscript

NIH-PA Author Manuscript

NIH-PA Author Manuscript

chromatography to give **17** (132 mg, 72%). ^{1}H NMR ($CDCl_3$): δ 1.29–1.39 (m, 4H), 1.53–1.59 (m, 2H), 163 (p, 2H, *J* = 6.8 Hz), 2.21 (t, 2H, *J* = 7.6 Hz), 2.32 (s, 3H, C*H*$_3$COS), 2.54 (t, 2H, *J* = 5.6 Hz), 2.85 (t, 2H, *J* = 7.6 Hz), 3.42–3.46 (m, 2H), 3.57 (t, 2H, *J* = 5.2 Hz), 3.64–3.67 (m, 20 H), 3.74 (t, 2H, *J* = 5.2 Hz), 4.07 (d, 2H, *J* = 5.2 Hz); ^{13}C NMR ($CDCl_3$): δ 25.6, 28.5, 28.8, 29.1, 29.4, 30.7, 36.5, 39.4, 41.6, 67.1, 70.0, 70.1, 70.27, 70.33, 70.4, 70.47, 70.50, 70.52, 70.6, 174.0, 196.2; HRMS $[C_{26}H_{48}N_2O_{11}S + Na]^+$: calc. 619.288, found: 619.288; Anal. Calcd for $C_{26}H_{48}N_2O_{11}S$: C 52.33; H 8.11; N 4.69, found: C 52.02; H 7.89; N 4.71.

3.6. *N*-(2-(2-hydroxyethylamino)-2-oxoethyl)-1-(7-mercaptoheptanamido)-3,6,9,12,15,18-hexaoxahenicosan-21-amide (19)

Compound **17** (97 mg, 163 μmol) was dissolved in CH_2Cl_2 (1 mL), a solution of 0.5 M HOBt in DMF (976 μL, 488 μmol) and DIPCDI (61 mg, 488 μmol) were added and the obtained mixture was stirred for 10 min. 2-Amino-ethanol (30 μL, 488 μmol) was added and the reaction was stirred for 18 h. After concentration, the residue was filtered through a silica column (gradient from hexane to 10% MeOH in EtOAc) and the crude product was dissolved in 10% hydrazine hydrate in EtOH (3 mL). The solution was stirred for 16 h, concentrated and azeotroped with toluene. The residue was dissolved in water (1 mL) containing dithiothreitol (10 mg), stirred under argon for 14 h and then filtered through a reversed phase column to give **19** (91 mg, 85%). ^{1}H NMR ($CDCl_3$): δ 1.14 (p, 2H, *J* = 7.2 Hz), 1.23 (p, 2H, *J* = 7.2 Hz), 1.41–1.47 (m, 4H), 2.10 (t, 2H, *J* = 7.6 Hz), 2.38 (t, 2H, *J* = 7.2 Hz), 2.46 (t, 2H, *J* = 6.0 Hz), 2.78 (s, 2H), 2.89 (s, 2H), 3.23 (t, 2H, *J* = 5.6 Hz), 3.46 (t, 2H, *J* = 5.6 Hz), 3.53–3.54 (m, 24H), 3.65 (t, 2H, *J* = 6.0 Hz), 3.76 (s, 1H), 3.94 (s, 1H); ^{13}C NMR ($CDCl_3$): δ 23.6, 25.2, 27.1, 27.5, 32.8, 35.6, 38.8, 40.8, 41.4, 66.5, 68.8, 69.3, 69.4, 69.46, 69.53, 169.8, 174.1, 176.9; HRMS $[C_{26}H_{51}N_3O_{10}S + Na]^+$: calc. 620.319, found: 620.311.

3.7. General procedure for synthesis of peptides/glycopeptides

Rink Amide AM Resin (33 μmol loading) was used for all peptides. All common amino acids were coupled on an Applied Biosystems 433A Peptide Synthesizer using HBTU–HOBt–DIEA with NMP as solvent and piperidine for Fmoc-deprotection. Coupling of the glycosylated amino acid (1*R*,2*S*)-*N*-Fmoc-1-amino-1-carboxypropan-2-yl 2,3,4,6-tetra-*O*-acetyl-β-D-galactoporanosyl-(1→3)-2-acetamido-4,6-*O*-benzylidene-2-deoxy-α-D-galactopyranoside and the linker **17** to the *N*-terminus was performed by dissolving the acid in DMF followed by addition of HOBt (2 eq.) and DIPCDI (2 eg.). This was stirred for 30 min, added to the resin and the resin was then shaken for 5–6 h. Another portion of HOBt (5 eq.) and DIPCDI (5 eq.) were added and the resin was shaken for an additional 18 h. Removal of the sugar and thioacetate groups was performed on the resin by treatment with 10% hydrazine hydrate in EtOH for 18 h. The peptides were cleaved by treating the resin with a solution of 2.5% 1,2-ethanedithiol and 2.5% water in TFA for 2 h. The peptide was then precipitated by pouring the TFA solution into ice-cooled Et_2O (10 mL) where upon the peptides precipitated. The obtained mixture was centrifuged and the organic phase removed. The residue was purified by HPLC (water–acetonitrile gradient, each containing 0.1% TFA) yielding the pure peptide/glycopeptides as a white solid.

3.7.1 HS-linker-TSSASTGHATPLPVTD (11)—Following the general procedure yielded **11** (43 mg, 63%). ^{1}H NMR (selected data) ($CDCl_3$): δ 2.38 (t, 2H, *J* = 6.8 Hz), 2.47 (t, 2H, *J* = 6.0 Hz), 2.71 (dt, 1H, *J* = 7.6 Hz, *J* = 16.8 Hz), 2.76 (dt, 1H, *J* = 5.6 Hz, *J* = 17.2 Hz), 2.98 (dd, 1H, *J* = 8.4 Hz, *J* = 15.6 Hz), 3.14 (dd, 1H, *J* = 5.6 Hz, *J* = 15.6 Hz), 3.23 (t, 2H, *J* = 5.6 Hz), 3.46 (t, 2H, *J* = 5.2 Hz), 3.65 (t, 2H, *J* = 6.0 Hz), 3.87 (s, 2H), 4.57 (dd, 1H, *J* = 5.2 Hz, *J* = 7.6 Hz), 7.14 (d, 1H, *J* = 1.2 Hz), 8.47 (d, 1H, *J* = 1.2 Hz); HRMS $[C_{88}H_{150}N_{21}O_{34}S]$: calc. 2077.04, found: 2077.04.

NIH-PA Author Manuscript

NIH-PA Author Manuscript

NIH-PA Author Manuscript

3.7.2. HS-linker-TSSASTGHAT(Galβ1→3GalNAcα)PLPVTD (12)—Following the general procedure yielded **13** (38 mg, 47%). ^{1}H NMR (selected data) ($CDCl_3$): δ 2.38 (t, 2H, *J* = 6.8 Hz), 2.47 (t, 2H, *J* = 6.0 Hz), 2.71 (dt, 1H, *J* = 7.6 Hz, *J* = 16.8 Hz), 2.76 (dt, 1H, *J* = 5.6 Hz, *J* = 17.2 Hz), 2.98 (dd, 1H, *J* = 8.4 Hz, *J* = 15.6 Hz), 3.14 (dd, 1H, *J* = 5.6 Hz, *J* = 15.6 Hz), 3.23 (t, 2H, *J* = 5.6 Hz), 3.35 (t, 1H, *J* = 2.0 Hz, *J* = 7.6 Hz), 3.46 (t, 2H, *J* = 5.2 Hz), 3.65 (t, 2H, *J* = 6.0 Hz), 3.87 (s, 2H), 4.74 (d, 1H, J = 3.6 Hz, GalNAc H-1^I), 7.15 (d, 1H, *J* = 1.2 Hz), 8.47 (d, 1H, *J* = 1.2 Hz); HRMS [$C_{102}H_{173}N_{22}O_{44}S$]: calc. 2442.170, found: 2442.170.

3.7.3. HS-linker-TSSAST(Galβ1→3GalNAcα)GHATPLPVTD (13)—Following the general procedure yielded **12** (41 mg, 51%). ^{1}H NMR (selected data) ($CDCl_3$): δ 2.38 (t, 2H, *J* = 6.8 Hz), 2.47 (t, 2H, *J* = 6.0 Hz), 2.71 (dt, 1H, *J* = 7.6 Hz, *J* = 16.8 Hz), 2.76 (dt, 1H, *J* = 5.6 Hz, *J* = 17.2 Hz), 2.98 (dd, 1H, *J* = 8.4 Hz, *J* = 15.6 Hz), 3.14 (dd, 1H, *J* = 5.6 Hz, *J* = 15.6 Hz), 3.23 (t, 2H, *J* = 5.6 Hz), 3.35 (t, 1H, *J* = 2.0 Hz, *J* = 7.6 Hz), 3.46 (t, 2H, *J* = 5.2 Hz), 3.65 (t, 2H, *J* = 6.0 Hz), 3.87 (s, 2H), 4.78 (d, 1H, *J* = 3.6 Hz, GalNAc H-1^I), 7.15 (d, 1H, *J* = 1.2 Hz), 8.47 (d, 1H, *J* = 1.2 Hz); HRMS [$C_{102}H_{173}N_{22}O_{44}S$]: calc. 2442.170, found: 2442.170.

Supplementary Material

Refer to Web version on PubMed Central for supplementary material.

Acknowledgments

The authors thank Anil Patri, Jeff Clogston and Jiwen Zheng of the Nanotechnology Characterization Laboratory (DLS data and analysis) and Kunio Nagashima and Jason de la Cruz of the Image Analysis Laboratory (TEM data and analysis) for their work and helpful discussions. Part of this work was supported by the Intramural Research Program of the National Cancer Institute.

References

1. Sonvico F, Dubernet C, Colombo P, Couvreur P. Curr. Pharm. Des 2005;11:2091–2105.
2. Thorek DLJ, Chen A, Czupryna J, Tsourkas A. Ann. Biomed. Eng 2006;34:23–38. [PubMed: 16496086]
3. Fu AH, Gu WW, Larabell C, Alivisatos AP. Curr. Opin. Neurobiol 2005;15:568–575. [PubMed: 16150591]
4. Barrientos AG, de la Fuente JM, Rojas TC, Fernandez A, Penades S. Chemistry-A European Journal 2003;9:1909–1921.
5. de la Fuente JM, Barrientos AG, Rojas TC, Rojo J, Canada J, Fernandez A, Penades S. Angew. Chem. Int. Ed 2001;40:2257–2261.
6. de Paz JL, Ojeda R, Barrientos AG, Penades S, Martin-Lomas M. Tetrahedron-Asymmetry 2005;16:149–158.
7. Rojas TC, de la Fuente JM, Barrientos AG, Penades S, Ponsonnet L, Fernandez A. Advanced Materials 2002;14:585–588.
8. Rojo J, Diaz V, de la Fuente JM, Segura I, Barrientos AG, Riese HH, Bernade A, Penades S. Chembiochem 2004;5:291–297. [PubMed: 14997521]
9. Daniel MC, Astruc D. Chem. Rev 2004;104:293–346. [PubMed: 14719978]
10. Grabar KC, Freeman RG, Hommer MB, Natan MJ. Anal. Chem 1995;67:735–743.
11. Robinson A, Fang JM, Chou PT, Liao KW, Chu RM, Lee SJ. Chembiochem 2005;6:1899–1905. [PubMed: 16149042]
12. Sun XL, Cui WX, Haller C, Chaikof EL. Chembiochem 2004;5:1593–1596. [PubMed: 15515080]
13. Chen YF, Ji TH, Rosenzweig Z. Nano Letters 2003;3:581–584.
14. de la Fuente JDM, Penades S. Tetrahedron-Asymmetry 2005;16:387–391.

NIH-PA Author Manuscript

NIH-PA Author Manuscript

NIH-PA Author Manuscript

15. Svarovsky, SA.; Barchi, JJ, Jr. De Novo Synthesis of Biofunctional Carbohydrate-Encapsulated Quantum Dots. In: Demchenko, AV., editor. Frontiers in Modern Carbohydrate Chemistry. 960 ed.. New York, NY: Oxford University Press; 2007. p. 375-394.
16. El-Boubbou K, Gruden C, Huang X. J. Am. Chem. Soc 2007;129:13392–13393. [PubMed: 17929928]
17. Ito M, Suzuki E, Naiki M, Sendo F, Arai S. Int. J. Cancer 1984;34:689–697. [PubMed: 6209227]
18. Hakomori SI. Adv. Cancer Res 1989;52:257–331. [PubMed: 2662714]
19. Hakomori S, Zhang YM. Chemistry & Biology 1997;4:97–104. [PubMed: 9190292]
20. Ojeda R, de Paz JL, Barrientos AG, Martin-Lomas M, Penades S. Carbohydr. Res 2007;342:448–459. [PubMed: 17173881]
21. Springer GF. Crit. Rev. Oncog 1995;6:57–85. [PubMed: 8573608]
22. Zanetti M, Lenert G, Springer GF. Int. Immunol 1993;5:113–119. [PubMed: 7680895]
23. Cao Y, Stosiek P, Springer GF, Karsten U. Histochem. Cell Biol 1996;106:197–207. [PubMed: 8877380]
24. Dziadek S, Kunz H. Chemical Record 2004;3:308–321. [PubMed: 14991920]
25. Dziadek S, Hobel A, Schmitt E, Kunz H. Angew. Chem. Int. Ed 2005;44:7630–7635.
26. Xu YF, Sette A, Sidney J, Gendler SJ, Franco A. Immunol. Cell Biol 2005;83:440–448. [PubMed: 16033540]
27. Glinsky VV, Glinsky GV, Rittenhouse-Olson K, Huflejt ME, Glinskii OV, Deutscher SL, Quinn TP. Cancer Res 2001;61:4851–4857. [PubMed: 11406562]
28. Khaldoyanidi SK, Glinsky VV, Sikora L, Glinskii AB, Mossine VV, Quinn TP, Glinsky GV, Sriramarao P. J. Biol. Chem 2003;278:4127–4134. [PubMed: 12438311]
29. Yu LG, Andrews N, Zhao Q, McKean D, Williams JF, Connor LJ, Gerasimenko OV, Hilkens J, Hirabayashi J, Kasai K, Rhodes JM. J. Biol. Chem 2007;282:773–781. [PubMed: 17090543]
30. Svarovsky SA, Szekely Z, Barchi JJ. Tetrahedron: Asymmetry 2005;16:587–598.
31. Brust M, Walker M, Bethell D, Schiffrin DJ, Whyman R. J. Chem. Soc. Chem. Commun 1994:801–802.
32. Brust M, Fink J, Bethell D, Schiffrin DJ, Kiely C. J. Chem. Soc., Chem. Commun 1995:1655–1656.
33. Lin CC, Yeh YC, Yang CY, Chen GF, Chen YC, Wu YC, Chen CC. Chem. Commun 2003:2920–2921.
34. de Souza AC, Halkes KM, Meeldijk JD, Verkleij AJ, Vliegenthart JFG, Kamerling JP. E. J. Org. Chem 2004:4323–4339.
35. Carvalho de Souza A, Halkes KM, Meeldijk JD, Verkleij AJ, Vliegenthart JFG, Kamerling JP. Chembiochem 2005;6:828–831. [PubMed: 15770624]
36. Fifis T, Mottram P, Bogdanoska V, Hanley J, Plebanski M. Vaccine 2004;23:258–266. [PubMed: 15531045]
37. Fifis T, Gamvrellis A, Crimeen-Irwin B, Pietersz GA, Li J, Mottram PL, McKenzie IFC, Plebanski M. J. Immunol 2004;173:3148–3154. [PubMed: 15322175]
38. Hollingsworth MA, Swanson BJ. Nat. Rev. Cancer 2004;4:45–60. [PubMed: 14681689]
39. Choudhury A, Moniaux N, Winpenny JP, Hollingsworth MA, Aubert JP, Batra SK. J. Biochem. (Tokyo) 2000;128:233–243. [PubMed: 10920259]
40. Andrianifahanana M, Moniaux N, Schmied BM, Ringel J, Friess H, Hollingsworth MA, Buchler MW, Aubert JP, Batra SK. Clin. Cancer Res 2001;7:4033–4040. [PubMed: 11751498]
41. Khorrami AM, Choudhury A, Andrianifahanana M, Varshney GC, Bhattacharyya SN, Hollingsworth MA, Kaufman B, Batra SK. J. Biochem. (Tokyo) 2002;131:21–29. [PubMed: 11754731]
42. Choudhury A, Moniaux N, Ulrich AB, Schmied BM, Standop J, Pour PM, Gendler SJ, Hollingsworth MA, Aubert JP, Batra SK. Br. J. Cancer 2004;90:657–664. [PubMed: 14760381]
43. Liu XO, Atwater M, Wang JH, Huo Q. Colloids Surf., B 2007;58:3–7.

NIH-PA Author Manuscript

NIH-PA Author Manuscript

NIH-PA Author Manuscript

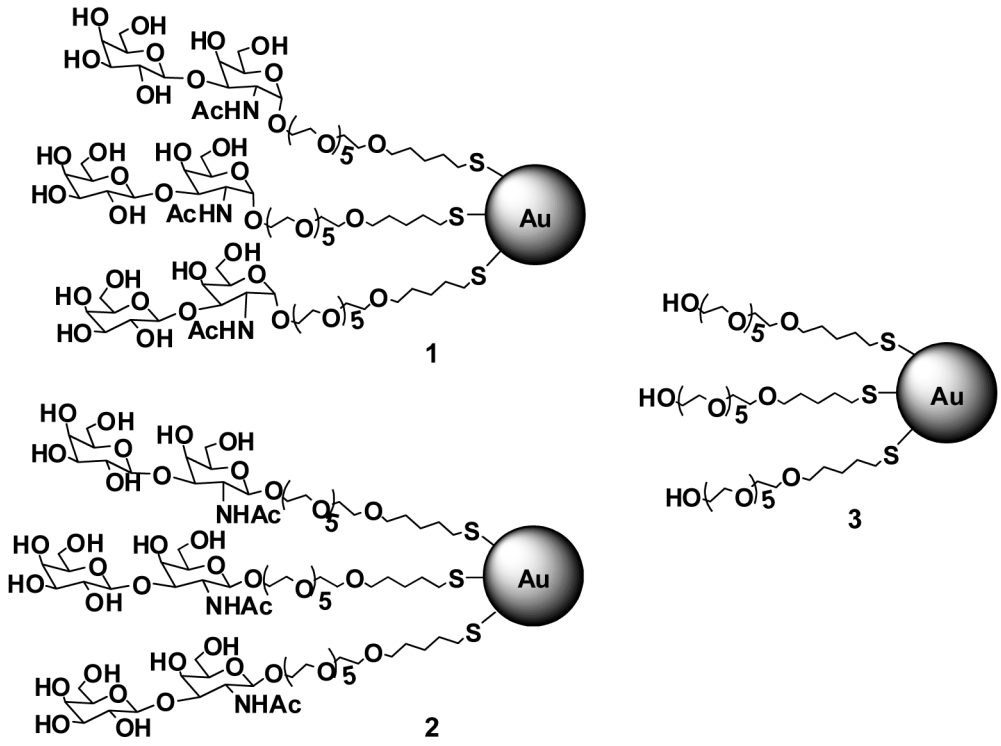

Figure 1.
TF_{ag} (**1**), β-TF_{ag} (**2**) and linker "control" (**3**) GNP's.

NIH-PA Author Manuscript
NIH-PA Author Manuscript
NIH-PA Author Manuscript

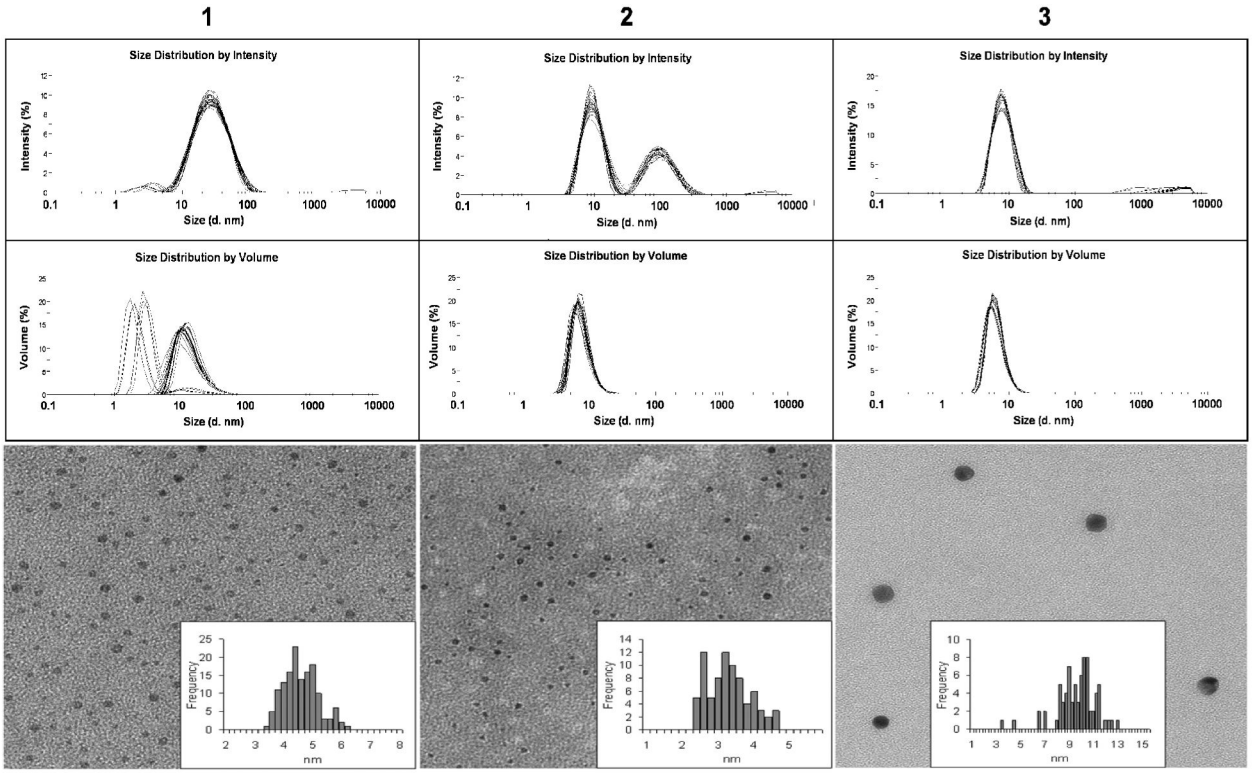

Figure 2.
DLS data for compounds **1**–**3**. Top trace is intensity vs. size while the bottom traces are volumes vs. size. The lower row shows TEM data for each NP with size histograms as an inset.

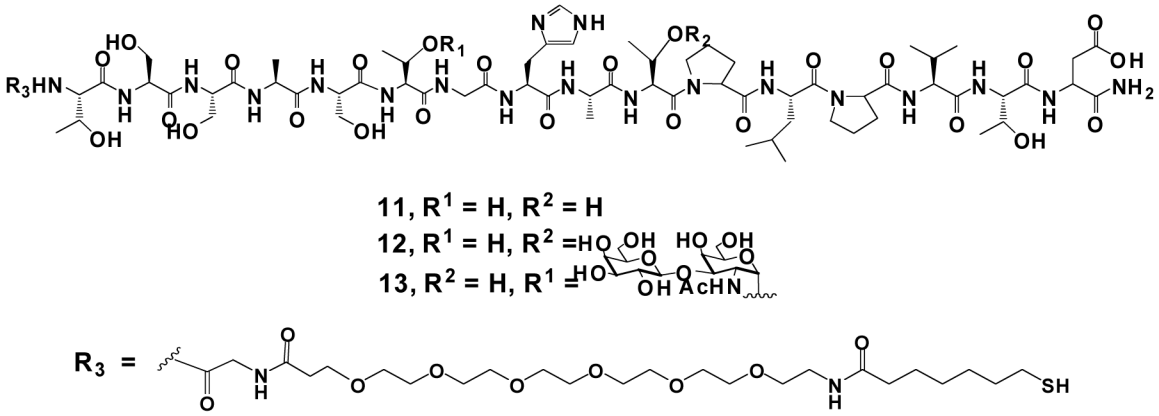

Figure 3.
Structure of $MUC4_{16}$ peptide and two glycopeptides with TF_{ag} at positions Thr^{6} and Thr^{10}. The linker R_3 was used to functionalize the N-terminus of the glycopeptide for GPNP synthesis.

NIH-PA Author Manuscript NIH-PA Author Manuscript NIH-PA Author Manuscript

NIH-PA Author Manuscript
NIH-PA Author Manuscript
NIH-PA Author Manuscript

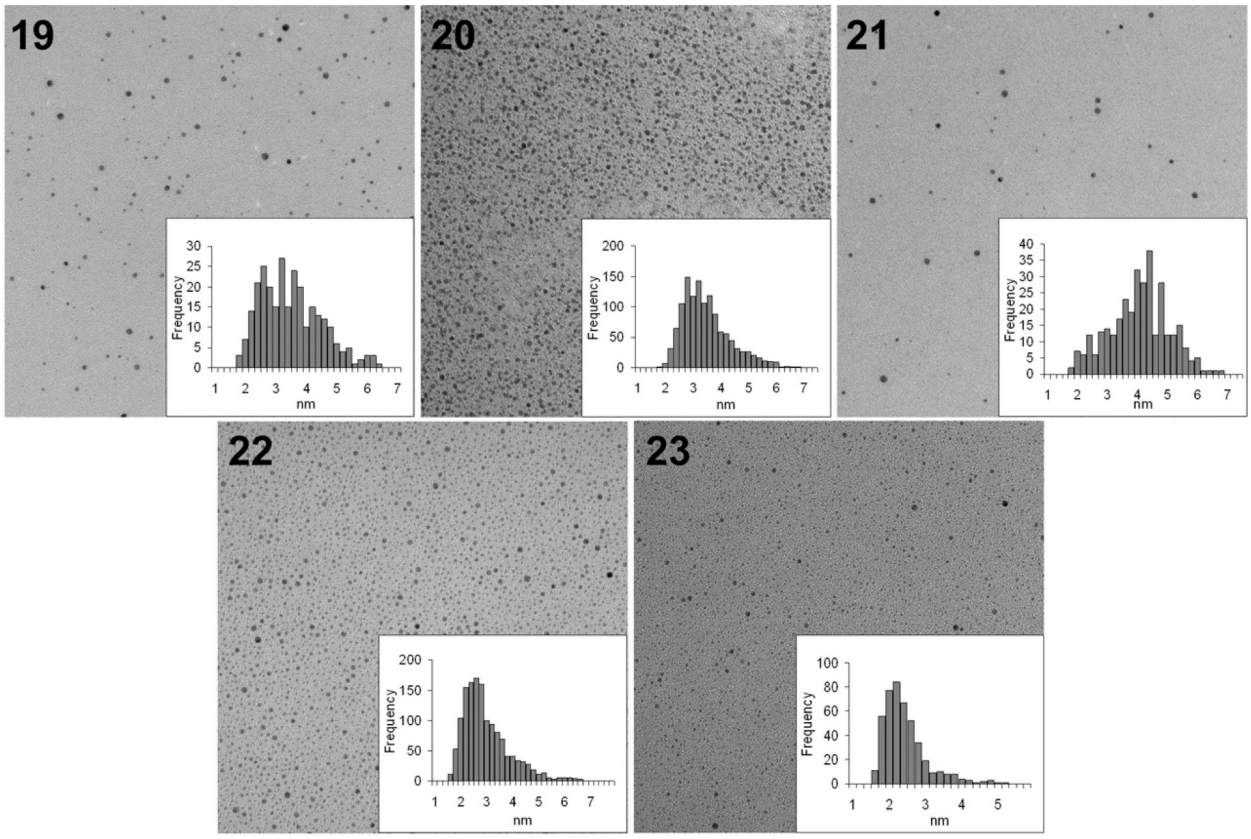

Figure 4.
TEM data for GPNP, peptide- and linker-coated NP's **19–23**.

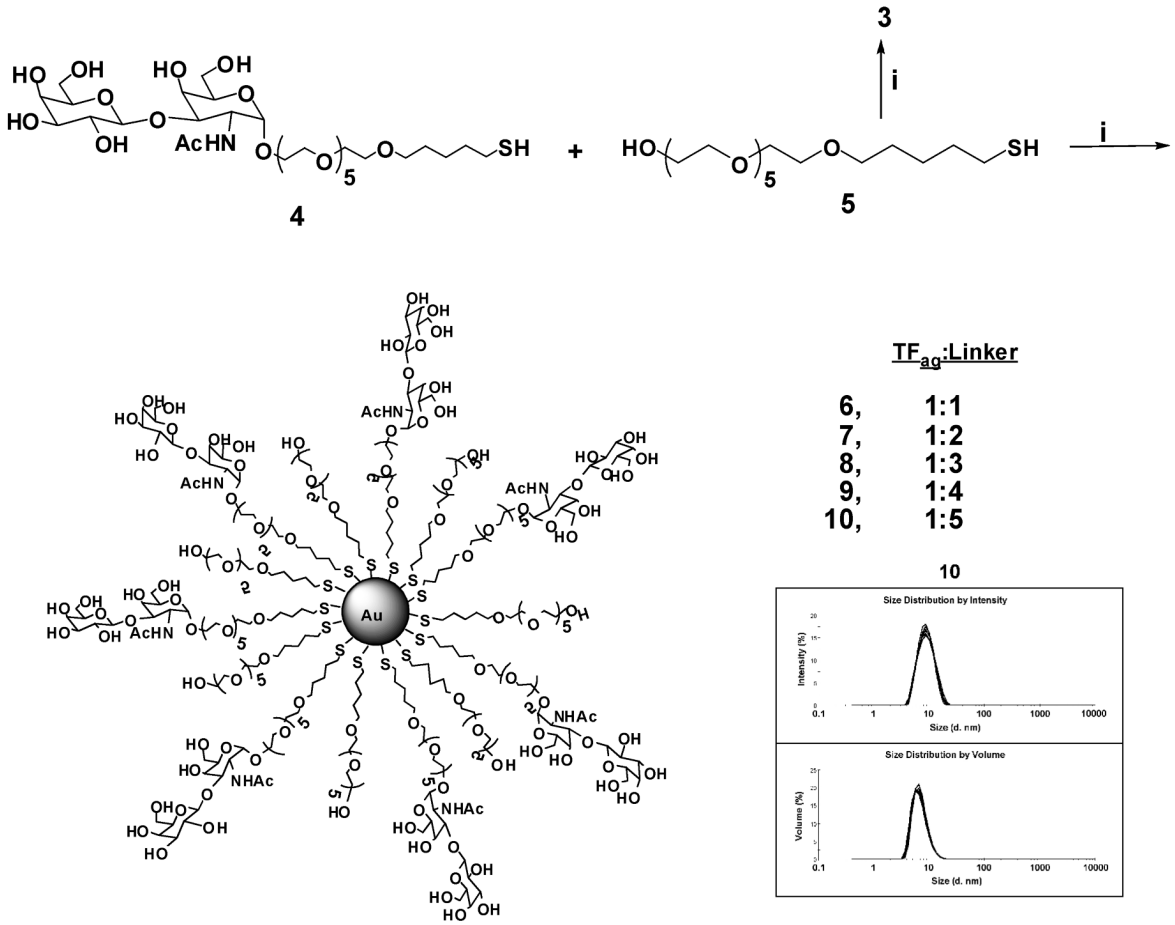

Scheme 1.

i) $HAuCl_4$, $NaBH_4$, H_2O, 0 °C; DLS data for compound **10** is shown in the lower right with intensity vs. size shown in the top trace and volume vs. size in the bottom trace.

NIH-PA Author Manuscript NIH-PA Author Manuscript NIH-PA Author Manuscript

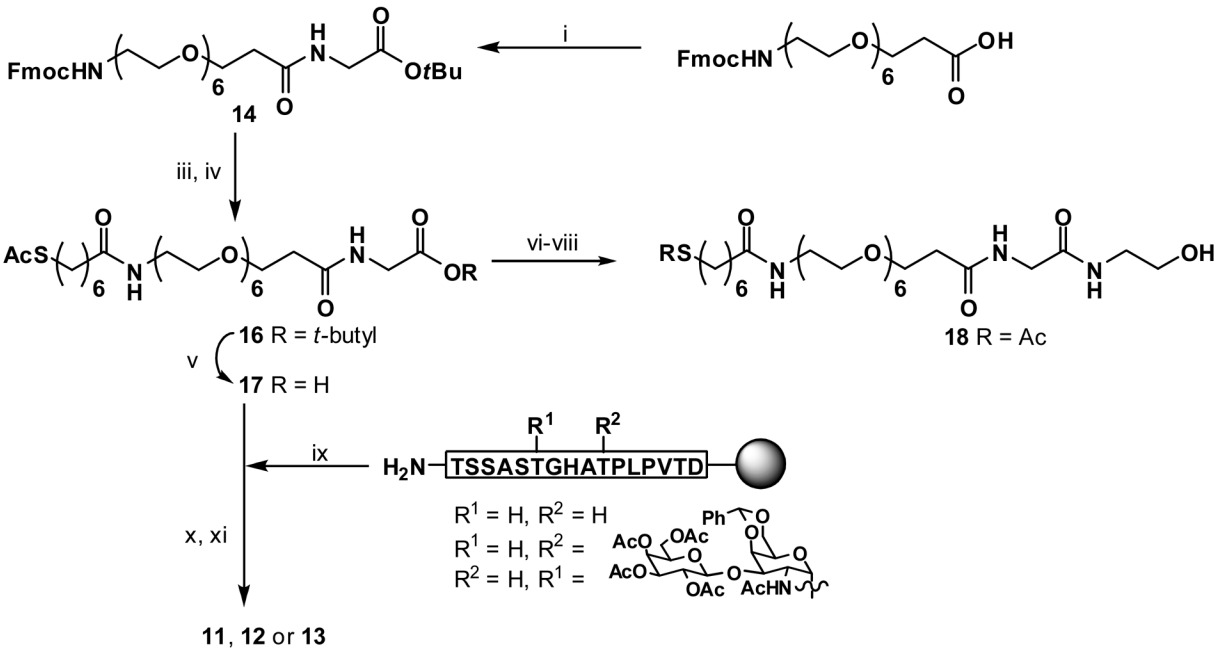

Scheme 2.

i) DIPCDI, HOBt, DMF, dichloromethane (CH_2Cl_2), 86%; ii) Thiolacetic acid, AIBN, 84%; iii) Piperidine, CH_2Cl_2; iv) $AcS(CH_2)_6COOH$ (**15**), DIPCDI, HOBt, DMF, CH_2Cl_2, 86% in two steps; v) TFA, 72%; vi) 2-Amino ethanol, DIPCDI, HOBt, DMF, CH_2Cl_2; vii) Hydrazine hydrate, EtOH; viii) Dithiothreitol, water, 85% in three steps; ix) **17**, DIPCDI, HOBt, DMF; x) Hydrazine hydrate, EtOH; xi) 95% TFA, 2.5% 1,2-ethanedithiol.

NIH-PA Author Manuscript NIH-PA Author Manuscript NIH-PA Author Manuscript

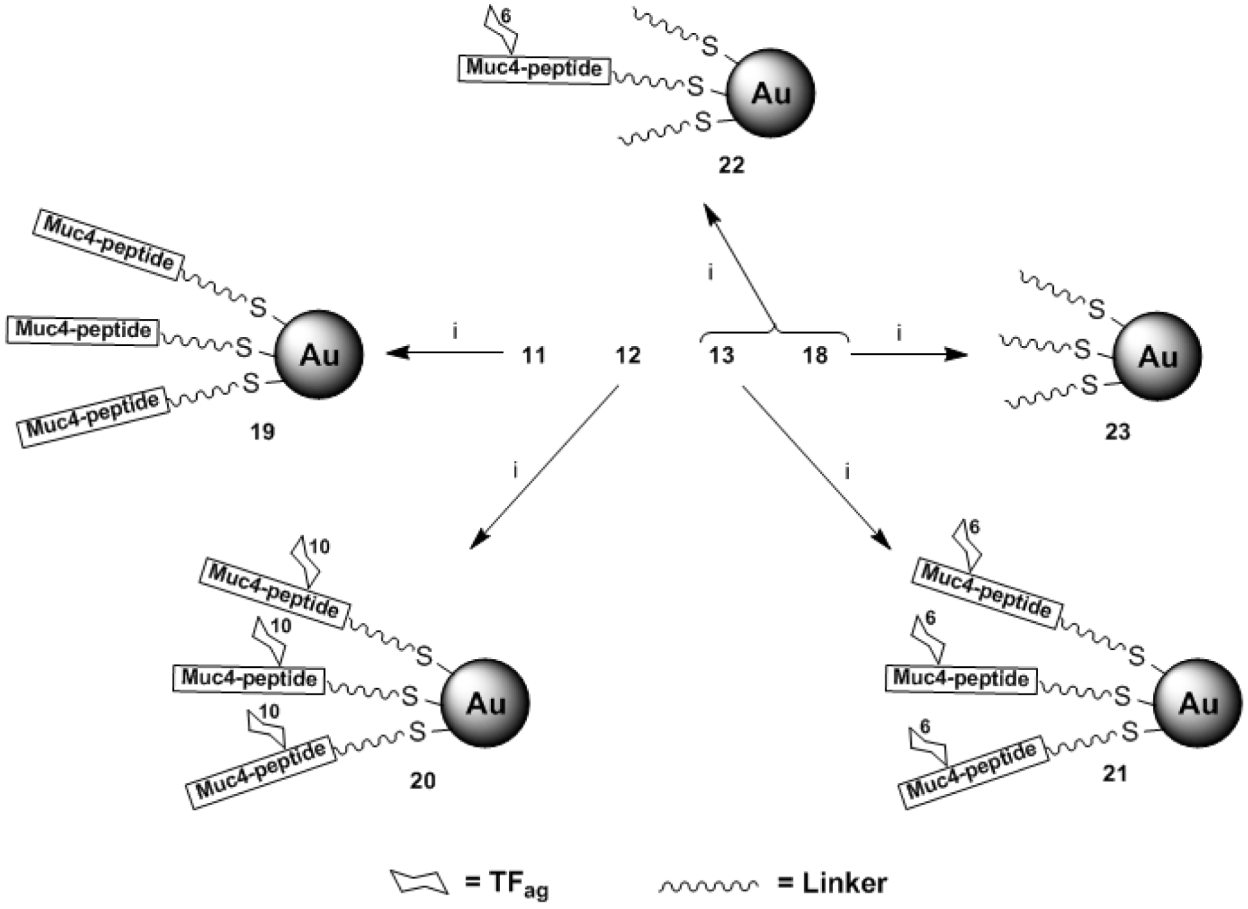

Scheme 3.
i) $HAuCl_4$, $NaBH_4$, H_2O, 0 °C.

NIH-PA Author Manuscript
NIH-PA Author Manuscript
NIH-PA Author Manuscript